In Situ Characterization of Mn(II) Oxidation by Spores of the Marine *Bacillus* sp. strain SG-1

John R. Bargar *,[1], Bradley M. Tebo[2], and John E. Villinski[3]

[1]Stanford Synchrotron Radiation Laboratory, SLAC, Stanford, CA 94309. E-mail: bargar@ssrl.slac.stanford.edu; Phone: (650)-926-4949; FAX: (650)-926-4100. [2]Marine Biology Research Division, Scripps Institution of Oceanography, 9500 Gilman Dr., La Jolla, CA 92093-0202. [3]Department of Hydrology and Water Resources, P.O. Box 210011, University of Arizona, Tucson, AZ 85721-0011.

*Author to whom correspondences should be addressed.

Abstract

Microbial oxidation of Mn(II) and subsequent precipitation of insoluble, reactive Mn(IV) oxides are primary sources of these solid phases in the environment and key controls on Mn cycling in natural waters. We have performed *in situ* x-ray absorption near-edge structure (XANES) spectroscopic measurements of Mn(II) oxidation by spores of the marine *Bacillus* sp. strain SG-1 to characterize the intermediates and products of the oxidation reactions. Mn(IV)-oxides resembling δ-MnO_2 were observed to form at a rapid rate (within 14 minutes of reaction onset). Mn(III) intermediates did not occur above detection limit (5 to 10% of total Mn), even though Mn(III)/(II,III) oxides (MnOOH or Mn_3O_4) should have been more stable than MnO_2 under the conditions of the experiments. These results suggest that Mn(IV) is the primary product of bacterial Mn(II) oxidation by *Bacillus* strain SG-1 and, by comparison to previous measurements in biotic systems, Mn(III)-oxides result from abiotic, autocatalytic oxidation of Mn(II) on surfaces of Mn(IV) oxides. Given that SG-1 is a good model for Mn(II)-oxidizing bacteria, these findings help to explain the predominance of Mn(IV)-oxides in aquatic environments.

1. INTRODUCTION

Microbial oxidation of Mn(II) occurs at rates up to 5 orders of magnitude greater than abiotic Mn(II) oxidation (Tebo, 1991; Tebo et al., 1997). The resulting Mn(III,IV) oxides are ubiquitous in natural waters as grains and grain coatings, have high sorptive capacities for metal ions, and oxidize many toxic organic and inorganic contaminants including aromatic hydrocarbons, Cr(III), Co(II), and hydrogen sulfide (Jenne, 1967; Huang, 1991; Post, 1999). Thus, Mn(II)-oxidizing bacteria impact the biogeochemical cycling of a large number of essential and toxic trace constituents of natural waters. In spite of their importance, the molecular mechanisms of these transformations at microbe-water interfaces are poorly understood.

Previous investigations have generated seemingly conflicting evidence regarding the existence of Mn(III) oxides as intermediates in Mn oxidation. Hem and Lind (1983) proposed that abiotic oxidation of Mn(II) leads to Mn(III) or mixed Mn(II,III) solid phase intermediates, which disproportionate to Mn(II)(aq) and Mn(IV) oxides. In this model, Mn(IV) oxides do not form at high pH (> 8) and Mn(II) concentrations > 10^{-6} M because the Mn(II,III) solid phase intermediates are stable with respect to disproportionation. In general support of this model, Hastings and Emerson (1986) reported the occurrence of hausmannite (Mn_3O_4) as an intermediate in Mn(IV) formation by spores of marine *Bacillus* sp. strain SG–1, and Mann et al. (1988) observed hausmannite as a product of Mn(II) oxidation by purified spore coats. In contrast to these observations, x-ray diffraction studies of SG–1 oxidation products (Mandernack et al., 1995) have showed that Mn(IV) solid phases were formed under the same pH and Mn(II) concentrations where Hem and Lind (1983) and Murray et al. (1985) observed Mn(III) minerals that only slowly aged to Mn(IV). XAFS spectroscopic measurements of Mn in lake sediments (Wehrli et al., 1995; Friedl et al., 1997) showed only evidence for Mn(II) and Mn(IV), which the authors took as permissive evidence for a one-step Mn(II) → (IV) oxidation process. However, transient formation of short-lived Mn(III) oxides or Mn(III)-enzyme complexes may not have

been detected in these studies. Time-resolved spectroscopic measurements of reaction progress spanning the reaction sequence in carefully chosen and chemically constrained model systems are required to resolve the mechanism of Mn(II) $\rightarrow$ (IV) oxidation.

In this communication we report results of *in situ* studies of the relative rates and reaction products of Mn(II) oxidation by the *Bacillus* sp. strain SG–1 using XANES spectroscopy. This technique provides quantitative information regarding Mn oxidation state, physical form, and host-phase identity *via* non-invasive measurements integrated over the whole sample.

2. EXPERIMENTAL METHODS

Mn K-edge XANES were measured at room temperature at the Stanford Synchrotron Radiation Laboratory beam line 4-1. Purified spores of the marine *Bacillus* sp. strain SG–1 were prepared according to published procedures (Rosson and Nealson, 1982) except that spores were also washed with 0.3–1mM ascorbate (10mM HEPES [4-(2-hydroxyethyl)-1-piperazineethanesulfonic acid] buffer) to remove Mn(III,IV) oxides formed during culturing. Samples were prepared in batch and in an *in situ* flow-through reaction cell that allowed collection of x-ray spectra during reaction (Villinski et al., 1999). Batch and flow-through supernatants/influents contained 50 mM NaCl in Milli-Q water buffered at pH 7.7 to 7.8 using 10 mM HEPES. Batch samples (10^{12}–10^{13} spores/L in air-equilibrated buffer) were prepared in 15 mL polypropylene centrifuge tubes. 1 mM Mn(II) was added to start the batch incubations and tubes were sealed and gently agitated for specific durations (*cf.*, Table 1). Reaction was halted by addition of 10 mM sodium azide and/or by placing samples in an ice bath, and spectra were measured immediately thereafter. Flow-through samples were prepared by agitating SG–1 spores in anoxic 5 mM $MnCl_2$ solution for 1 to 6 hrs. to preadsorb Mn(II). The reacted spores were loaded into the flow-through cell anaerobically, and a spectrum was recorded (top-most bolded curve at 6553 eV in Fig. 1). A 25 µL/min. inflow of air-equilibrated 100 µM Mn(II)

solution was then initiated, and spectra were measured continuously throughout the ensuing oxidation reaction. If Mn(II) oxidation proceeds by the two-step mechanism of Hem and Lind, then formation of hausmannite or one of the MnOOH polymorphs should have been thermodynamically favored over MnO_2 under initial bulk solution conditions (Mandernack et al., 1995). Spectra from samples were fit with linear combinations of component spectra using a non-linear least-squares algorithm in EXAFSPAK (George, 1993). Binding energies were allowed to float during fits, and >90% of fits had energy shifts less than 0.15 eV. No energy shifts exceeded 0.47 eV. No more than five components were included in any fit. Component spectra included: clean SG-1 spores (signal is from intracellular Mn(II)), $MnCl_2(aq)$, Mn(II) adsorbed on SG-1, Mn(IV) reaction products isolated at the end of the reaction, manganite (γ-MnOOH), groutite (α-MnOOH), feitknechtite (β-MnOOH), bixbyite ($(Mn,Fe)_2O_3$), hausmannite (Mn_3O_4), aqueous Mn(III)pyrophosphate (assumed to be $MnHP_2O_7(aq)$), solid Mn(III)-phthalocyanine chloride, Mn(III)-acetyl acetonate, Mn(III)-tetra(4-pyridyl)porphine chloride, protein-bound Mn(III,IV) (oxygen-evolving complex of photosystem II (Riggs-Gelasco et al., 1996)), hollandite (α-MnO_2$), pyrolusite ($\beta$-MnO_2$), nsutite (γ-MnO_2$), todorokite $((Na,Ca,K)(Mg,Mn)Mn_6O_{14} \cdot 5H_2O)$, and birnessite $((Na,Ca,K)(Mg,Mn)-Mn_5O_{12} \cdot H_2O)$.

3. RESULTS AND DISCUSSION

Figure 1 shows Mn K-edge spectra as a function of reaction progress for Mn(II) oxidation by SG-1 measured *in situ* during reaction. The maximum absorption features for Mn(II) and Mn(IV) occur as sharp peaks at *ca*. 6553 eV and 6562 eV, respectively. Neither Mn(II) nor Mn(IV) in these samples have peaks in the region 6556 to 6560 eV. In contrast, Mn(III) often exhibits strong peaks or shoulders in this energy region (Villinski et al., 1999) (*cf.*, Fig. 2). The spectrum of clean spores (dotted spectrum in Fig. 1) has a Mn(II) signal from intracellular (insoluble) Mn(II) and no Mn(III) or Mn(IV) peaks.

As Mn(II) oxidation was initiated, a Mn(IV) peak (6562 eV) appeared and grew with time. Simultaneously, the amplitudes of Mn(II) peaks at 6553, 6569, and 6594 eV decreased. Isosbestic points (constant absorbance) at *ca.* 6558 and 6584 eV suggest that two components, *i.e.*, Mn(II) and Mn(IV), dominate the samples. Fit results for spectra measured at 14, 154, 349, and 545 min. (Table 1) indicate that Mn(IV) occurred in the samples within 14 min. of reaction. After 545 min. (top-most bolded curve at 6562 eV in Fig. 1), approximately half of Mn in the sample was present as Mn(IV). No peaks corresponding to Mn(III) are visible in Fig. 1, and in no cases did addition of Mn(III) model spectra to the fits improve matches to sample spectra. The detection limit for Mn(III) is estimated at 5 to 10%, based on fits to spectra containing admixtures of Mn(III) components. Hence, we conclude that Mn(III) was not present at or above this concentration at any time during the reaction.

XANES spectra from batch samples (Fig. 2a) provide information about Mn(II) oxidation in the absence of continuous x-ray exposure. As with the flow-through experiment, reaction progress was characterized by the growth of a Mn(IV) peak at 6562 eV and the diminution of Mn(II) peaks. Fits to batch sample spectra (Table 1) were not improved by addition of Mn(III) components. This point is illustrated in Figure 2b, which shows that both the edge and pre-edge spectra of the final SG-1 oxidation products matches that of synthetic δ-MnO$_2$. The SG-1 product edge is dissimilar to the spectra from a number of Mn(III) compounds, including manganite and hausmannite (previously reported to occur in similar systems (Hem and Lind, 1983; Mandernack et al., 1995)), and MnHP2O7(aq), which provides an example for Mn(III) species lacking long-range order. This comparison suggests that the SG-1 oxidation products are δ-MnO$_2$ (vernadite). This conclusion is consistent with EXAFS measurements of SG-1 oxidation products from incubations covering a range of temperatures, ionic strengths, and Mn concentrations (Bargar et al., 2000).

Mn(III)-bearing oxides expected to occur in this system, including hausmannite, manganite, and feitknechtite, have been shown to be very slow to disproportionate (months to

years) into MnO_2 (Hastings and Emerson, 1986; Hem and Lind, 1983; Mandernack et al., 1995). For example, Mandernack (1995) showed that 3-month incubations of hausmannite (at 25° and 55° C) resulted in no significant disproportionation. This behavior is inconsistent with the observation that Mn(IV) oxide formation occurred rapidly and without detection of Mn(III) in our samples. Hence, we conclude that bulk Mn(III)-oxides did not occur as intermediates in our samples in the fashion proposed by Hem and Lind (1983).

Van Waasbergen *et al*. (1996) concluded that Mn(II) is oxidized by a multicopper oxidase protein (MnxG) in spores of SG-1. Since known multicopper oxidases catalyze one-electron oxidation of their substrates (da Silva and Williams, 1991), this observation suggests that microbial Mn(IV) oxide formation occurs via two successive one-electron transfer reactions. Ehrlich (1996) suggested that Mn(III) occurs as an oxidation intermediate, and is enzyme-oxidized to Mn(IV). The presence of such molecular Mn(III) intermediates in our samples cannot be ruled out because they could have occurred below the detection limit of the technique. The same statement applies to Mn(III)-oxide surface coatings present at sub-monolayer-equivalent concentrations. If 10% of Mn in the system (*i.e.*, the detection limit) were present as a Mn(III) surface coating on δ-MnO_2 (present as, *e.g.*, 33% of Mn in the system), then an estimate of about one monolayer equivalent surface concentration of Mn(III) on δ-MnO_2 is obtained for the detection limit (based on a surface area of 224 m^2/g for the biogenic oxides (Nelson et al., 1999) and using the MnO_2 (110) crystallographic truncation as a model surface, which has 10.4 Mn sites/nm^2). If either protein-bound or sub-monolayer surface-coating Mn(III) intermediates did occur in our samples, then the absence of their spectral components implies that: (i) the Mn(III) $\rightarrow$ (IV) step is fast; and (ii) the reaction is rate-limited by steps involving Mn(II), such as adsorption of Mn(II) to the spore surfaces, the concentration of oxidation-active surface sites, and/or the Mn(II) $\rightarrow$ (III) reaction step.

Hastings and Emerson (1986) and Mandernack et al. (1995) observed the presence of Mn(III)-bearing oxides in Mn(II)/SG-1 reaction products, and the former proposed them to be

intermediates in the Mn(II) $\rightarrow$ (IV) oxidation reaction. This conclusion is in apparent contradiction to the present results. However, the techniques used in these previous studies (XRD, electron microscopy, average oxidation state measurements) are relatively insensitive to amorphous phases and/or provide only indirect measurement of oxidation states of individual phases in heterogeneous systems. Therefore, amorphous Mn(IV) oxides could have been present as primary phases but escaped recognition. In general, samples in these previous studies were incubated for periods of time (0.6 days to several months) longer than encompassed by the present measurements. Based on this comparison, we propose that Mn(III)-bearing oxides observed in previous microbial oxidation studies may have initially formed via abiotic, autocatalytic oxidation of Mn(II) on Mn(IV)-oxide surfaces over time scales of hours to days, analogous to the formation of Mn(III) (oxyhydr)oxides on Fe oxide surfaces (Junta and Hochella, 1994). Subsequent to this process, autocatalytic oxidation also could have occurred on Mn(III)-oxide surfaces. A key component of this idea is the observation that hausmannite and/or one of the MnOOH polymorphs should have been more stable than Mn(IV) oxides in many of these previous measurements (Mandernack et al., 1995), which would have provided a driving force for Mn(II) oxidation to Mn(III) minerals *via* abiotic pathways.

4. CONCLUSIONS

Mn(II) was rapidly oxidized to Mn(IV) oxides in the presence of *Bacillus* sp. strain SG-1, in spite of the fact that hausmannite and/or Mn(III) oxyhydroxides should have been more stable than MnO_2. Based on the ability to describe the spectra as linear combinations of Mn(II) and Mn(IV) oxides, and the absence of Mn(III) spectral features, we conclude that bulk Mn(III) oxides did not occur as reaction intermediates. Trace concentrations of complexed Mn(III) species and/or Mn(III)-oxide coatings cannot be ruled out as intermediates. We propose that bulk Mn(III) oxides previously observed in other studies may have formed initially as a result of abiotic, autocatalytic oxidation of Mn(II) at Mn(IV)-oxide surfaces. The rapid bacterial

oxidation of Mn(II) to Mn(IV) oxides provides an explanation for the predominance of Mn(IV) oxides in aquatic environments (*cf.*, Mandernack et al. (1995))**.**

5. ACKNOWLEDGMENTS

6. REFERENCES

Bargar J. R., Tebo B. M., Pecher K. H., Chiu V., Villinski J. E., and Tonner B. M. (2000) Kinetics and Products of Mn Oxide Biomineralization by Spores of the Marine Bacillus sp. strain SG-1. In *Preprints of Extended Abstracts, Division of Environmental Chemistry, 220th ACS National Meeting, Washington, DC, August 2000.* American Chemical Society (in press).

da Silva J. J. R. F. and Williams J. P. (1991) *The Biological Chemistry of the Elements*. Clarendon Press.

Ehrlich H. L. (1996) How microbes influence mineral growth and dissolution. *Chemical Geology* **132**, 5-9.

Friedl G., Wehrli B., and Manceau A. (1997) Solid phases in the cycling of manganese in eutrophic lakes: New insights from EXAFS spectroscopy. *Geochimica et Cosmochimica Acta* **61**(2), 275-290.

George G. N. (1993) EXAFSPAK. Stanford Synchrotron Radiation Laboratory.

Hastings D. and Emerson S. (1986) Oxidation of manganese by spores of a marine Bacillus: kinetic and thermodynamic considerations. *Geochimica et Cosmochimica Acta* **50**, 1819-1824.

Hem J. D. and Lind C. J. (1983) Nonequilibrium models for predicting forms of precipitated manganese oxides. *Geochimica et Cosmochimica Acta* **47**, 2037-2046.

Huang P. M. (1991) Kinetics of redox reactions on manganese oxides and its impact on environmental quality. In *Rates of Soil Chemical Processes* (ed. D. L. Sparks and D. L. Suarez), pp. 191-230. Soil Science Society of America, Inc.

Jenne E. A. (1967) Controls on Mn, Fe, Co, Ni, Cu and Zn concentrations in soils and water: the significant role of hydrous Mn and Fe oxides. In *Trace Inorganics in Water*, pp. 337 - 387. American Chemical Society, Washington, D.C.

Junta J. L. and Hochella M. F. (1994) Manganese(II) oxidation at mineral surfaces: A microscopic and spectroscopic study. *Geochimica et Cosmochimica Acta* **58**(22), 4985-4999.

Mandernack K. W., Post J., and Tebo B. M. (1995) Manganese mineral formation by bacterial spores of the marine *Bacillus* strain SG-1: Evidence for the direct oxidation of Mn(II) to Mn(IV). *Geochim. Cosmochim. Acta* **59**, 4393-4408.

Mann S., Sparks N. H. C., Scott G. H. E., and deVrind-deJong E. W. (1988) Oxidation of manganese and formation of Mn_3O_4 (hausmannite) by spore coats of a marine Bacillus sp. *Applied Environmental Microbiology* **54**, 2140-2143.

Murray J. W., Dillard J. G., Giovanoli R., Moers H., and Stumm W. (1985) Oxidation of Mn(II): Initial mineralogy, oxidation state and aging. *Geochimica et Cosmochimica Acta* **49**, 463-470.

Nelson Y. M., Lion L. W., Ghiorse W. C., and Shuler M. L. (1999) Production of biogenic Mn oxides by Leptothrix discophora SS-1 in a chemically defined growth medium and evaluation of their Pb adsorption characteristics. *Applied and Environmental Microbiology* **65**, 175-180.

Post J. E. (1999) Manganese oxide minerals: crystal structures and economic and environmental significance. *Proceedings of the National Academy of Sciences USA* **96**, 3447-3454.

Riggs-Gelasco P. J., Mei R., Yokum C. F., and Penner-Hahn J. E. (1996) Reduced derivatives of the manganese cluster in the oxygen-evolving complex of photosystem II; an EXAFS study. *Journal Amer. Chem. Soc.* **118**, 2387-2399.

Rosson R. A. and Nealson K. H. (1982) Manganese binding and oxidation by spores of a marine *Bacillus*. *Journal of Bacteriology* **151**, 1027-1034.

Tebo B. M. (1991) Manganese(II) oxidation in the suboxic zone of the Black Sea. *Deep-Sea Research* **38**(Suppl. 2), S883-S905.

Tebo B. M., Ghiorse W. C., van Waasbergen L. G., Siering P. L., and Caspi R. (1997) Bacterially-mediated mineral formation: Insights into manganese(II) oxidation from molecular genetic and

biochemical studies. In *Geomicrobiology: Interactions Between Microbes and Minerals.*, Vol. 35 (ed. J. F. Banfield and K. H. Nealson), pp. 225-266. Mineralogical Society of America,.

van Waasbergen L. G., Hildebrand M., and Tebo B. M. (1996) Identification and characterization of a gene cluster involved in manganese oxidation by spores of the marine *Bacillus* sp. strain SG-1. *Journal of Bacteriology* **178**, 3517-3530.

Villinski J. E., O'Day P. A., Corley T. L., and Conklin M. H. (1999) A flow-through cell for *in situ*, real time x-ray absorption spectroscopy studies of geochemical reactions. In *U.S. Geological Survey Toxic Substances Hydrology Program-- Proceedings of the Technical Meeting. Charleston, South Carolina, March 8-12, 1999, Volume 1, Contamination from Hard Rock Mining.* (ed. D. W. Morganwalp and H. T. Buxton), U.S. Geological Survey Water-Resources Investigations Report 99-4018, pp. 217-225.

Wehrli B., Friedl G., and Manceau A. (1995) Reaction rates and products of manganese oxidation at the sediment-water interface. In *Aquatic Chemistry: Interfacial and Interspecies Processes*, Vol. 244 (ed. C. P. Huang, C. R. O'Melia, and J. J. Morgan), pp. 111-134. Am. Chem. Soc.

Table 1. Linear least-squares combination fits of components to spectra. Estimated standard deviations are given in parentheses.
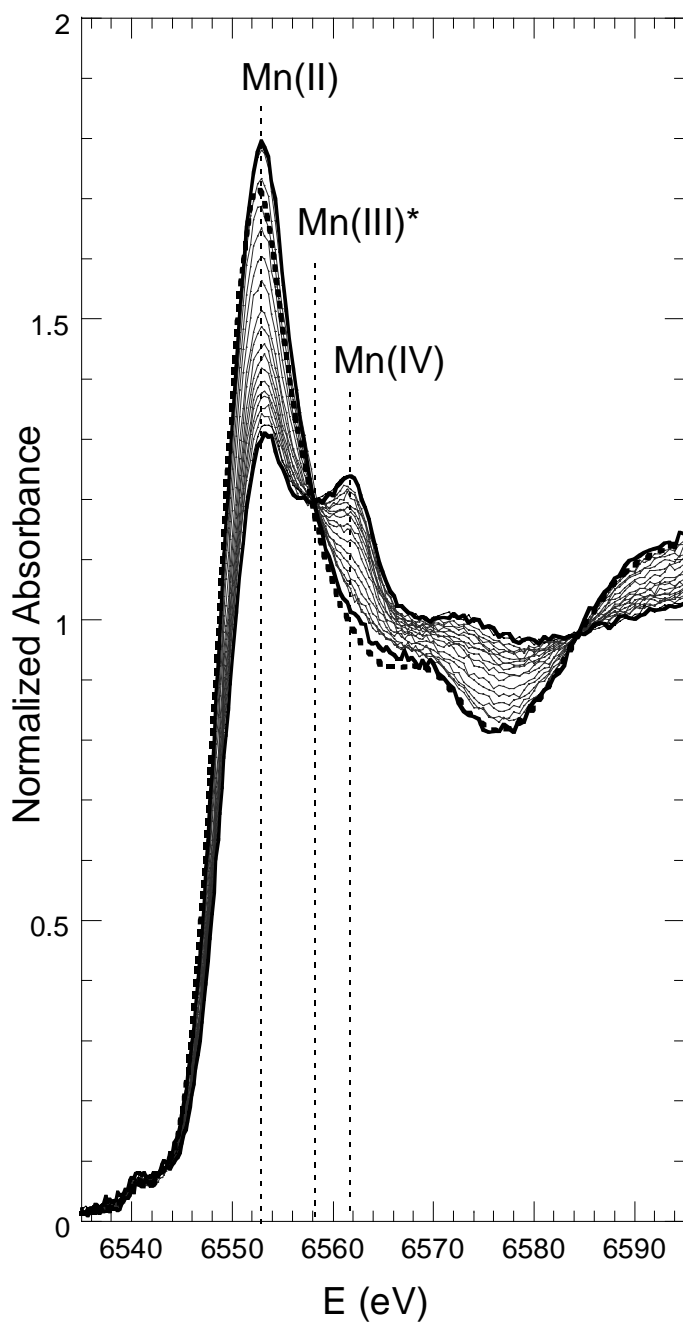
Sample	Reaction Time (min.)	Fit Components (fractional contribution)				Sum	Residual
		Clean Spores	Mn(IV)	Aq Mn(II)	Adsorbed Mn(II)		
Batch 1	30	0.731 (0.005)	0.185 (0.0007)	0.074 (0.005)	0.015 (0.005)	1.005	5.11E-6
Batch 2	60	0.643 (0.006)	0.291 (0.0008)	0.055 (0.006)	0.014 (0.006)	1.003	7.59E-6
Batch 3	155	0.557 (0.008)	0.367 (0.001)	0.060 (0.009)	0.018 (0.008)	1.002	1.35E-5
Batch 4	480	0.411 (0.013)	0.538 (0.001)	0.031 (0.011)	0.019 (0.009)	0.999	2.01E-5
Flow 1	14	0.816 (0.010)	0.030 (0.001)	0.146 (0.011)	0.017 (0.009)	1.009	2.31E-5
Flow 2	154	0.814 (0.011)	0.177 (0.001)	--	0.012 (0.011)	1.003	2.36E-5
Flow 3	349	0.671 (0.002)	0.319 (0.001)	--	0.011 (0.008)	1.001	2.00E-5
Flow 4	545	0.573 (0.002)	0.413 (0.001)	--	0.015 (0.008)	1.001	2.26E-5

FIGURE CAPTIONS

Figure 1. Normalized K-edge spectra as a function of time (up to 9.3 hr.) for Mn(II) + SG-1 *Bacillus* measured *in situ* using a flow-through cell. The dotted curve is the spectrum of clean spores. The time interval between spectra is about 28.0 min. The top- and bottom-most (at 6553 eV) bolded curves are the first and last spectra, respectively, for the reaction sequence. *The vertical dotted line labeled "Mn(III)" marks the approximate expected position of Mn(III) absorption edges, were they to be present (see Fig. 2).

Figure 2. a. Normalized K-edge spectra as a function of time for Mn(II) + SG-1 *Bacillus* batch samples. Dashed curves overlying spectra are fits. Fit components are shown as solid (Mn(II)) and dashed (Mn(IV)) curves below each spectrum. b. Spectra of Mn(II)/SG-1 final reaction products (labeled "SG-1") compared to model compounds: hausmannite ("Haus"), manganite ("Mang"), $MnHP_2O_7(aq)$ ("Pyro"), bixbyite ("Bixb"), and synthetic δ-MnO_2. Inset shows baseline-subtracted pre-edge details.

Bargar et al. Figure 2